RECOVERY OF FURTHER DATA FROM 1958 EPSILON

C. A. Lundquist, R. J. Naumann, and S. A. Fields[1]

(Paper presented at the COSPAR Conference, Florence, Italy, April 10 - 14, 1961)

[1]Research Projects Division, George C. Marshall Space Flight Center, Huntsville, Alabama.

ABSTRACT

15638

On satellite 1958 Epsilon, two of the detectors for trapped particle radiation were plastic scintillation counters which were mounted with their axes normal to the longitudinal axis of the satellite and such that the velocity vectors of most of the energetic particles counted made a small angle with the counter axes. As the satellite rolls and tumbles, the scintillator axes trace out a complex Lissajous figure in space. The counting rates exhibit very strong dependence on the direction of the counter axes. The rate has a maximum when the counter axes are perpendicular to the magnetic field. Previously published analyses of data from these counters were based primarily on these maximum values.

Particularly for the plastic scintillator, it is now possible to recover more useful data from the telemetered data from this counter through a determination of the direction of the counter axis as a function of time. This determination utilizes the antenna characteristics of the satellite transmitters, the strength of the signal received by ground stations, the phenomenological properties of the counting rate modulations, and the equations for rigid body motion. After the direction of the counter axis has been determined, the directional dependence of the radiation may be determined at points in the radiation belts.

Satellite 1958 Epsilon Résumé

Earth satellite 1958 Epsilon (Explorer IV), sketched in Fig. 1, had the pencil-like configuration characteristic of the first three Explorer satellites. As injected into orbit by a Juno I vehicle [1], the satellite was initially spinning with 12 revolutions per second about its long axis of symmetry. Immediately after injection, or probably even during burning of the final rocket stage, a small angle developed between the total angular momentum vector and the axis of symmetry of the satellite. In accord with the classical rigid body equations of motion, the axis of symmetry executed a force-free precession about the total angular momentum vector. In such a state of motion, periodic strains occurred within the not quite rigid satellite body. The net result of these strains was a slow dissipation of kinetic energy of rotation of the satellite without any change in its total angular momentum. This loss of energy, in turn, required that the angle between the symmetry axis and the angular momentum become larger. Thus, the satellite made a gradual transition toward a 90° angle between the body axis and the angular momentum vector. As this case is approached, angular motion about a transverse axis through the body is conventionally

referred to as tumble, and rotation about the symmetry axis as roll. This transition had been observed and discussed for Explorer I [2] and Explorer III even before the launch of Explorer IV.

Satellite 1958 Epsilon contained a radiation belt experiment prepared by James A. Van Allen and his associates at the State University of Iowa [3]. Two of the four radiation detectors were G-M counters whose response was relatively independent of direction. Data from these detectors have been discussed by several authors [3, 4, 5, 6, 7, 8]. The other two detectors were scintillation crystals placed beneath small circular holes in the steel cylindrical shell of the satellite. Radiation coming through these holes had to penetrate only a thin foil to reach the crystal, while the remaining primary radiation detected had to penetrate the steel wall of the satellite and such other matter as lay on its path to the detector. The collimating apertures were such that the area of the scintillator visible through the hole had its full value for a cone of half-angle 6° and fell linearly to zero for a 19° half-angle. Radiation capable of penetrating the thin foils over the scintillators, but not the shell of the satellite, consequently was counted only when its direction made a small angle with the axis of the counter.

The axis common to each hole, scintillator, and photomultiplier was

normal to the symmetry axis of the satellite. As the satellite tumbled and rolled, the directions of the counter axes traced out complex Lissajous figures in space. The direction of the counter axes relative to the magnetic field of the earth is particularly important, since the direction of trapped particle radiation is strongly dependent on the angle with the magnetic field. The radiation data from the scintillation detectors showed pronounced modulations having periods corresponding to the spin and tumble periods. The radiation rates had absolute maxima whenever the counter axes were perpendicular to the magnetic field. Previously published analyses of data from these counters were based primarily on these maximum values [3, 4, 8]. However, when the motion of the satellite is sufficiently well known, the directions of the scintillation counter axes may be determined as a function of time and more of the radiation data analyzed.

Empirical Determination of Satellite Orientation

The two modulations of the counting rate data from the plastic scintillator (detector A on 1958 Epsilon) are illustrated in the Channel 2 telemetry record in Fig. 2. Each telemetry switching cycle indicates the accumulation of 2048 pulses from the scintillator. The

modulations occurred only when the radiation rates were high enough that the switching period was small compared to the roll and tumble periods. The counts from the plastic scintillator were also carried on telemetry Channel 5 with a scaling factor of 16 instead of 2048. The total radiation energy deposited in a CsI crystal (detector B) was transmitted as a frequency deviation on temeletry Channel 4.

An absolute maximum occurred when the axis of either scintillation counter is orthogonal to the magnetic field, and absolute minimum when parallel to the magnetic field. Since the axis of the counter need not become orthogonal or parallel to the magnetic field during every tumble period, relative maxima and minima also occurred as the satellite rolled and tumbled.

One of the observed modulations occurred with a period of approximately 3½ seconds throughout the lifetime of the satellite. This modulation corresponds to one-half of the tumble period. The other modulation in the counting rate occurred with a period which varied from 0.04 seconds at injection on July 26, 1958 to 140 seconds on September 2, 1958. While other phenomena may cause modulations in the counting rate, the evidence now indicates clearly that this second modulation corresponds to one-half of the roll period.

Using this identification, a plot of the roll period as a function of time was prepared (Fig. 3), in which data were used from twenty different tracking stations located all over the world. The first portion of the curve, when the period was very short, was determined using Channel 4. The second portion of the curve was determined by data from Channel 2. A few points on the curve came from Channel 5. The smoothness of the curve, and the fact that the data came from many different locations, supports the conclusion that this is the true roll period.

From launch until August 28, 1958, the roll period had gradually increased, then it began decreasing. On August 29, 1958, after the roll period had decreased from more than 190 seconds to less than 30 seconds, it suddenly began increasing again. The period continued to increase until the transmitter ceased operation about September 3, 1958.

There is a possibility that the satellite reversed its roll direction on August 28, 1958, but this assumption is not supported by present data. The roll rate was plotted assuming that the satellite was rolling in a positive direction until reaching the peak of roll period and thereafter rolling in the negative direction. If the satellite reversed roll directions, one might expect a continuous curve through zero, but this

is apparently not the case. The suggestion that the roll decayed to a very low value and then somehow became accelerated again in the same direction seems to give a more reasonable curve than the assumption of roll reversal. A roll reversal could not possibly explain the minimum on August 29.

After the roll period reached one second, the angle between the angular momentum vector and the satellite symmetry axis was greater than 85°, and within the accuracy of the present discussion, the tumble axis may be identified with the angular momentum vector. With both the tumble and role rates known, the direction of the tumble axis in space must also be determined in order to obtain the counter axis orientations as a function of time. This determination was somewhat problematical since the satellite was not provided with any on-board sensors for this purpose. However, examination of the satellite antenna radiation patterns suggested a method whereby the look angle, or the angle which the line of sight from the tracking station to the satellite makes with the tumble axis, could be inferred from the recorded radio signal strength variations [9, 10] . Figure 4 shows these radiation patterns for the 108 mc/sec and 108.03 mc/sec transmitters carried on the satellite. It may be seen that the 108 mc/sec antenna,

being an asymmetrical dipole, has a minor lobe on either side of the nose of the satellite, whereas the 108.03 mc/sec antenna exhibits a characteristic dipole pattern. In either case, the radiation is linearly polarized in any plane containing the symmetry axis.

If the satellite is viewed along the tumble axis with a linearly polarized receiving antenna, fading will be observed at twice the tumble frequency due to the rotating plane of polarization of the emitted radiation. The plane of polarization is also rotated by the Faraday effect resulting from magneto-ionic splitting as the signal traverses the ionosphere. The rotation rate of the latter effect, which is due to the changing integrated electron density along the path of propagation as the satellite moves relative to the tracking station, is slow compared to the tumble rate for frequencies of 108 mc/sec and therefore does not materially change the observed patterns of signal strength variations. Thus, for the case where the look angle, Ψ , is small, that is, when the satellite is viewed almost along the tumble axis, the signal strength variations are essentially the same for both transmitters.

If the satellite is viewed in the plane of tumble, fades will occur in the 108.03 mc/sec signal strength patterns at twice the tumble frequency, due to the nulls in the antenna radiation pattern. These nulls

are indistinguishable from those due to polarization fading in the case of small Ψ ; consequently, the 108.03 mc/sec signal strength variations do not provide usable information if a linearly polarized tracking antenna is used. However, when viewing in the tumble plane, the small lobes on either side of the nose are apparent in the 108 mc/sec signal strength patterns. This distinguishing feature then enables one to determine whether the look angle Ψ is large or small. As it turns out, most of the signal strength recordings taken by the Huntsville tracking station contain the small lobes in the 108 mc/sec pattern. On two days, August 12 and 18, passes were observed in which the small lobes were absent for an interval of time during the pass. A simulation of the observed signal strength variations was performed on an analogue computer in which it was shown that the small lobes would be visible in the signal strength variations unless Ψ was less than about 20°.

The line of sight vector was computed at the times where the small lobes were absent on the August 12 and 18 passes. To facilitate the plotting of this vector, which shall be normalized and designated as $\vec{U}$, it is desirable to express it in terms of two position angles, i.e., right ascension and declination. Since the satellite is tumbling essentially in a plane, one should expect to observe the same signal

strength variations on either side of the plane, hence, the same pattern should be observed when looking along $\vec{U}$ as when looking along $-\vec{U}$. Therefore, the $\vec{U}$ is plotted as well as $-\vec{U}$ for each pass. Figure 5 is such a plot of the sight vector for two passes on August 12. the single lines indicate the orientations of the sight vector when the small lobes are visible in the signal strength recordings, hence $\Psi > 20°$. The double lines indicate the orientations of the sight vector when these lobes were absent, or when $\Psi < 20°$. The dashed line around the region where Ψ is observed to be less than 20° represents the intersection of a cone, whose half angle is 20°, and the celestial sphere. This fit is determined graphically and the axis of the cone is assumed to be parallel to the tumble axis. At this stage in the analysis, there is no way of determining the sense of tumble; hence, the angular momentum vector of the satellite may either be parallel or anti-parallel to the cone axis.

On August 18, the Huntsville tracking station altered their receiving antenna system. Instead of using a single dipole array, an attempt to obtain polarization diversity by adding another dipole array with crossed polarization was made. The two antenna arrays were mounted on separate pedestals, being separated by about 50 meters. Their outputs were added by a "T" junction and then detected by a single Hallamore receiver. As the satellite moved overhead, the path

length to the two antennas changed, thus altering the phase angle between the two antenna outputs. This produced an interferometer effect that altered the effective polarization of the receiving antenna. For example, if the two ouput voltages are in phase, the array is effectively plane polarized at 45° to each element. As the phase angle becomes 90°, the array becomes circularly polarized. The location of the antennas was such that the polarization change was usually slow compared to the tumble rate so that several tumble cycles could be observed at more or less constant polarization.

This technique allowed the use of 108.03 mc/sec signal strength patterns. The times when the antenna array was circularly polarized could be obtained by observing when the fades were less severe. At these times, the amplitude of the fades allowed an estimate of the look angle. Lack of calibration on the recorded signal strength records precluded an accurate measurement of the look angle, but a crude estimate could be made on the basis of comparison of the fading amplitude observed during the circularly polarized portion with the more severe fades observed when the antenna was linearly polarized. If the signal strength exhibited periods where little or no fading was evident, the look angle Ψ was estimated to be less than 30° . If the fading was

discernible, but still much less than the severe fades, Ψ was estimated to be between 30° and 45° . If the observed signal was a mixture of antenna radiation pattern fades and polarization fades, Ψ was estimated to be from 45° to 60° . If the pattern is predominately antenna radiation pattern fades, lessened only slightly as the polarization changes, Ψ is estimated to be 60° to 75° . If Ψ is between 75° and 90°, severe fades due to the radiation nulls along the nose and tail are observed regardless of the polarization of the receiving antenna. The tumble rate and phase may be determined quite accurately from the observations of the times of occurrences of these nose - tail fades. The tumble rate was observed to be 0.9103 rad/sec on August 27 and appeared to decrease linearly with time at the rate of 0.0016 rad/sec per day.

For days where a sufficient number of passes were available, the right ascension and declination of the sight vector at various times during the passes were plotted in the manner described previously. The type of signal strength variation noted was indicated by shading. A set of transparent overlays was prepared showing the intersections on the celestial sphere of a family of cones of various half-angles about an axis having a particular declination. These overlays were used to graphically determine the position of the tumble axis that best satisfied

the observed signal strength patterns; Fig. 6 shows a typical determination. The right ascension of the tumble axis could be fairly well determined by making use of the 75° to 90° patterns in the signal strength which appear to be fairly reliable. The declination is probably determined with less certainty.

The methods used for determining the tumble axis are admittedly crude, since the look angles could only be estimated. Graphical fitting was used primarily for expediency. While a more elegant numerical method might have been attempted, it was not felt justifiable in light of the crudeness of the data. Furthermore, it was necessary to use several passes during the same day to define sufficiently the tumble axis. Since the tumble axis may have shifted by as much as 10 degrees during this time, the best that can be hoped for is some mean location that may be considered effective for that day.

On certain passes during the month of September, the tracking station at Salisbury, South Rhodesia was able to eliminate the polarization fading by hand-rotating their linearly polarized antenna [11]. When this is possible, the line of sight must be nearly along the tumble axis so that the nose - tail fades will not be visible. Also, the sense of tumble may be determined by observing the direction of antenna rotation that will eliminate the fading.

Using the tumble axis orientation derived from the Huntsville tracking station data, the look angle for the Salisbury station was computed at the times fading could be eliminated by antenna rotation. In every case the look angle was small (less than 30°) when fading was successfully eliminated. This provides a consistent check on the determination of the tumble axis. The sense of rotation determined from the Salisbury data is consistent with the assumed sense of rotation that was required to explain the phase relationship between the observed counting rate peaks and the nose - tail fades in the Huntsville data.

The right ascensions and declinations of the tumble axis obtained by the methods described were plotted as a function of days after launch in Fig. 7. Using these data for the direction of the tumble axis, the average insolated area was calculated. Using the curves of predicted interior temperature for various insolated areas prepared by Snoddy [12], the expected temperatures were found as a function of time and compared with observed temperatures. These were found to be in satisfactory agreement.

Also, the average projected area normal to the velocity vector at perigee was computed. When this area was compared with the drag variations observed [13], the agreement was again satisfactory.

It is difficult to say how accurate the tumble axis determination actually is, although the success in explaining the observed temperature and the drag variations is encouraging. It is felt that the determination is generally good to about $\pm$ 10° in angular position with possibly somewhat higher uncertainty in declination during the times when the tumble axis lies near the equator. It can be shown that uncertainties of this magnitude do not seriously detract from the accuracy of obtaining count rate as a function of the angle the counter axis makes with the magnetic field lines.

Analytical Treatment of Satellite Orientation

The empirically determined body motions of the satellite 1958 Epsilon are indeed complicated. No simple explanation of the motions can be expected, and at present no complete explanation can be made. However, calculations have been made which shed some light on the problem.

In a study of the excursions of the total angular momentum vector, [14], the classical differential equations of motion were formulated using the four Euler parameters as generalized coordinates. Euler parameters rather than Euler angles or some other coordinates were chosen because of their convenience for numerical integration.

The gravitational effects on the satellite were the first studied in detail. Numerical integration of the equations of motion by Jerry Driggers and Joan Kassner, MSFC Computation Division, showed that excursions of the angular momentum of the order of one or two degrees per day result from the gravitational interaction. However, excursions as large as ten degrees per day are observed. Thus, the conclusion is reached that gravitational torques are significant and must be included in any complete treatment, but they are not the dominant effects. The further observation was first made by Charles Whitney of the Smithsonian Astrophysical Observatory that the direction of the motion induced by the gravitational torques is generally in the observed direction of motion.

The shell of the satellite and the case of the last stage rocket left attached as part of the satellite were both of 410 stainless steel. This steel has a residual flux density of 8 to 12 kilogausses from a 10 kilogauss applied field [15]. During testing of the satellite instrumentation, the payload portion of the satellite above the last stage rocket was placed on a vibration table. Strong magnetic fields are associated with the table, which might have left the shell permanently magnetized. A residual magnetization of about one-fifth of the residual flux density from 10 kilogausses would interact with the magnetic field

of the earth to give torques producing changes in the angular momentum direction on the order of 10°/day. However, the changes do not appear to be in the correct direction to explain the observed motion.

The other torques considered do not seem to yield appreciable torques.

Directional Dependence of Counting Rates

A convenient analytical representation of the direction of the counter axes relative to the magnetic field was given by Shelton [16] in a discussion of this problem. This representation assumed that the direction of the tumble axis, the tumble rate, the roll rate, and a set of initial tumble and roll phase angles are known at some selected initial time. Using these data and the analytical representation, the angle between the counter axes and the magnetic field is easily calculated as a function of time.

To analyze a particular telemetry record, the direction of the tumble axis is taken from the determination of this direction discussed earlier. The tumble and roll rates are determined with as much accuracy as possible, using the procedures previously described and the particular telemetry record. Finally, the tumble and roll phase angles are determined for an arbitrary time during the record, using a simple

fitting procedure.

A typical plot of the angle between the plastic scintillation counter axis and the magnetic field versus time is shown in Figure 8. Also shown are the counting rates for this scintillator during the same time interval. Breaks in this curve correspond to noise bursts where no data could be reduced. From the data in this last figure, Figs. 9-11 show counting rate versus counter angle with the magnetic field.

An analysis of this sort is limited to those situations where the telemetry switching period is small compared to the tumble and roll periods. Further, an extended period of telemetry reception relatively free from noise and signal fade-outs is required. Only a small fraction of the total data simultaneously satisfy these special conditions on counting rate and telemetry quality. A significant number of satisfactory cases do exist, and these have been analyzed.

From the counting rate curves like Fig. 9, the angular dependence of the radiation at various points in the radiation belts can be determined if the angular and energy responses of the counters are known with sufficient accuracy for various kinds of radiation. For such a study, a more detailed calibration of the counters is desired than required for previous studies. Such a calibration has been initiated using the spare satellite which was not launched.

Conclusions

The determination of the body motions of satellite 1958 Epsilon has made possible the recovery of further radiation belt information from the data transmitted by the satellite. The study of the body motions of such satellites has also been shown to pose interesting problems which demand further consideration.

REFERENCES

1. B. B. Greever, IRE Transactions on Military Electronics Vol. MIL-4 (1960).

2. A. R. Hibbs, "Scientific Results from the Explorer Satellites 1958 Alpha and Gamma," Jet Propulsion Lab Ext. Pub. 514 — presented at the 9th IAF Congress, Amsterdam 25-30 Aug. 1958.

3. J. A. Van Allen, C. E. McIlwain and G. H. Ludwig, "Radiation Observations with Satellite 1958 Epsilon," J. of Geophys. Res. 64 271 (1959).

4. J. A. Van Allen, C. E. McIlwain and G. H. Ludwig, "Satellite Observations of Electrons Artificially Injected into the Geomagnetic Field," J. of Geophys. Res. 64 877 (1959).

5. Y. Miyazaki and H. Takeuchi, "Radiation Measurements from Satellite 1958 Epsilon," Space Research, edited by H. Kallmann Bijl, 869 (1960) North-Holland Publishing Co., Amsterdam.

6. P. Rothwell and C. E. McIlwain, "Magnetic Storms and the Van Allen Radiation Belts: Observations from Satellite 1958 Epsilon," Space Research, edited by H. Kallmann Bijl, 897 (1960) North-Holland Publishing Co., Amsterdam.

7. E. C. Ray, "On the Theory of Protons Trapped in the Earth's Magnetic Field," J. of Geophys. Res. 65 1125 (1960).

8. J. A. Van Allen, "The Geomagnetically Trapped Corpuscular Radiation," J. of Geophys. Res. 64 1683 (1959).

9. T. A. Barr, "Explorer IV Antennas," Explorer IV - 1958 Epsilon Orbital Data Series, Issue 1, p. 3 (Aug. 1958), Army Ballistic Missile Agency and Smithsonian Astrophysical Observatory.

10. R. J. Naumann, "Recent Information Gained from Satellite Orientation Measurement," paper presented at the 4th Symposium on Ballistic Missile and Space Technology, UCLA, Los Angeles (1959).

11. Private communications with G. D. Wall, c/o Van Neikerk, Kleyn, and Edwards, Salisbury, Southern Rhodesia.

12. G. Heller, "Problems Concerning the Thermal Design of Explorer Satellites," IRE Transactions on Military Electronics, Vol. MIL-4, p. 109 (1960).

13. C. A. Whitney, "Atmospheric Densities from Explorer IV," Smithsonian Institution Astrophysical Observatory, Special Report No. 18, p. 15 (1958).

14. C. A. Lundquist, R. J. Naumann, "Orbital and Rotational Motion of a Rigid Satellite," Seminary Proceedings: Tracking Programs and Orbit Determination, Jet Propulsion Lab., Cal Inst. of Tech., Pasadena, Calif. (1960).

15. Metals Handbook, edited by T. Lyman, Amer. Soc. for Metals, Metals Park, Novelty, Ohio (1961), p. 794.

16. R. Shelton, "The Determination of the Directional Distribution of Charged Particles Trapped in the Magnetic Field of the Earth," paper presented to the Committee of AGARD, Paris, France (1959).

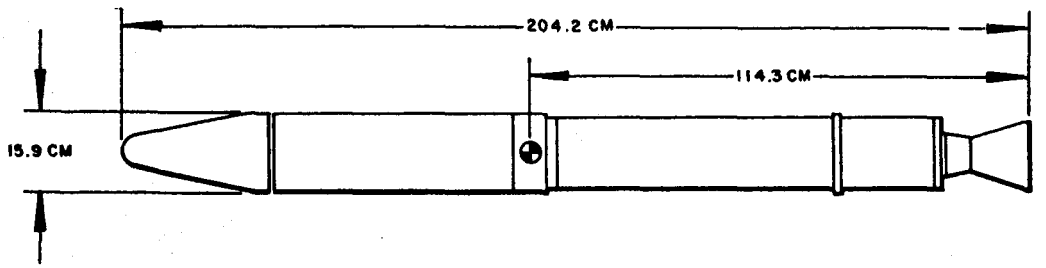

DATA

EMPTY WEIGHT	16.73 KG
POLAR MOMENT OF INERTIA	0.056×10^7 GM CM^2
TRANSVERSE MOMENT OF INERTIA	4.752×10^7 GM CM^2
FRONTAL AREA	198.06 CM^2
MAXIMUM PROJECTED AREA	2954.8 CM^2

FIG. 1 Explorer IV external configuration and dynamical properties.

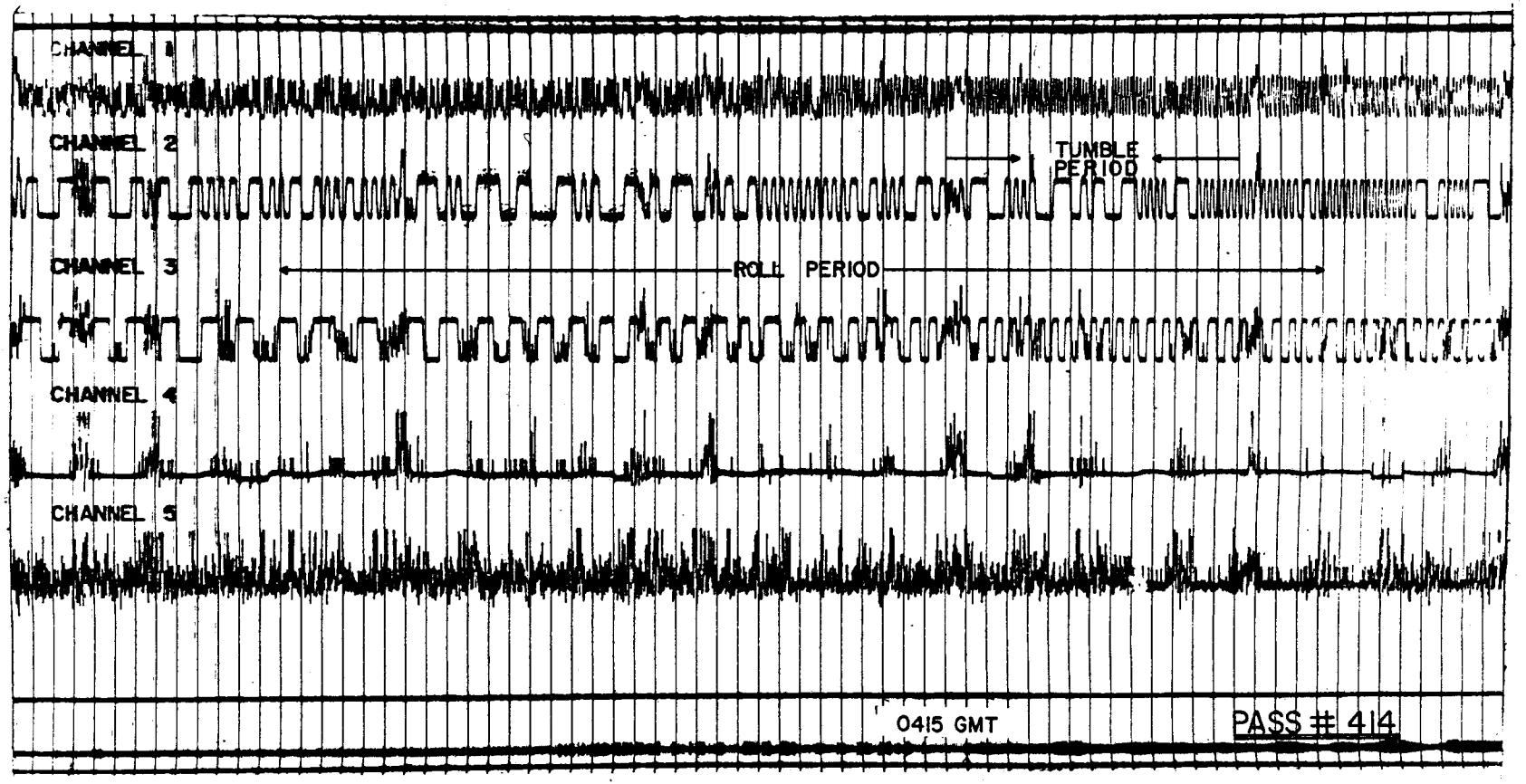

FIG. 2 Telemetry sample showing the variations in the Channel II counting rates due to the body motions of Explorer IV.

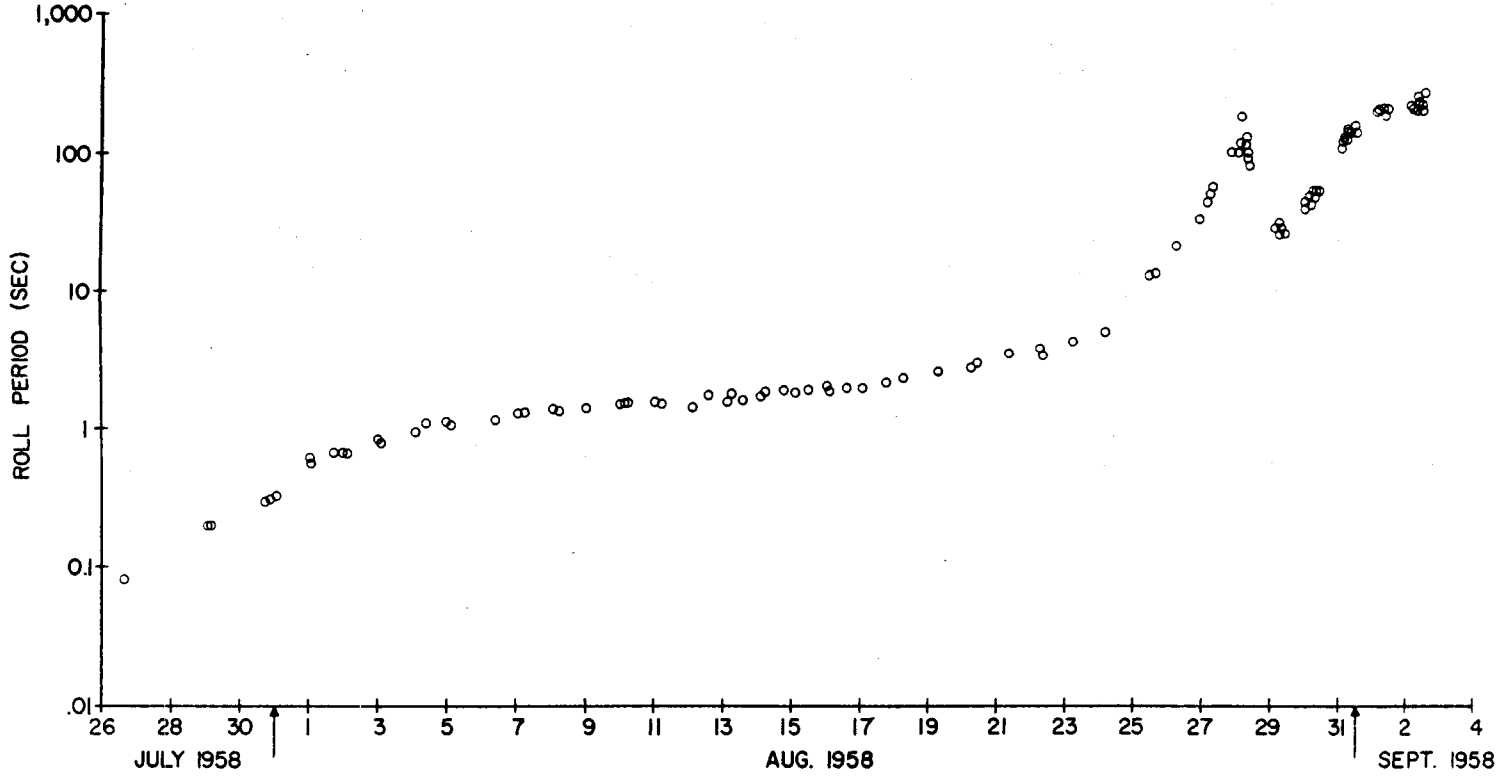

FIG. 3 Observed roll period during the telemetry lifetime of Explorer IV.

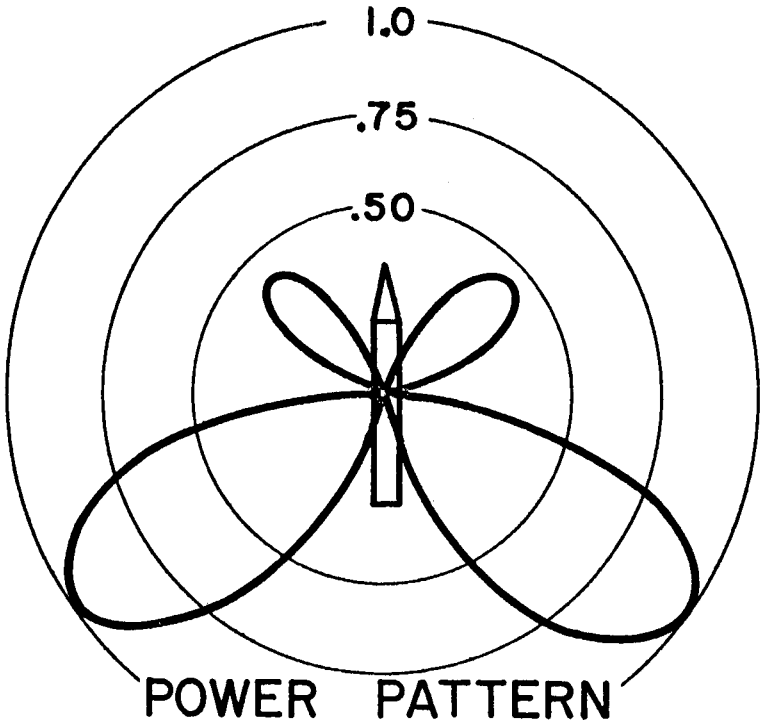

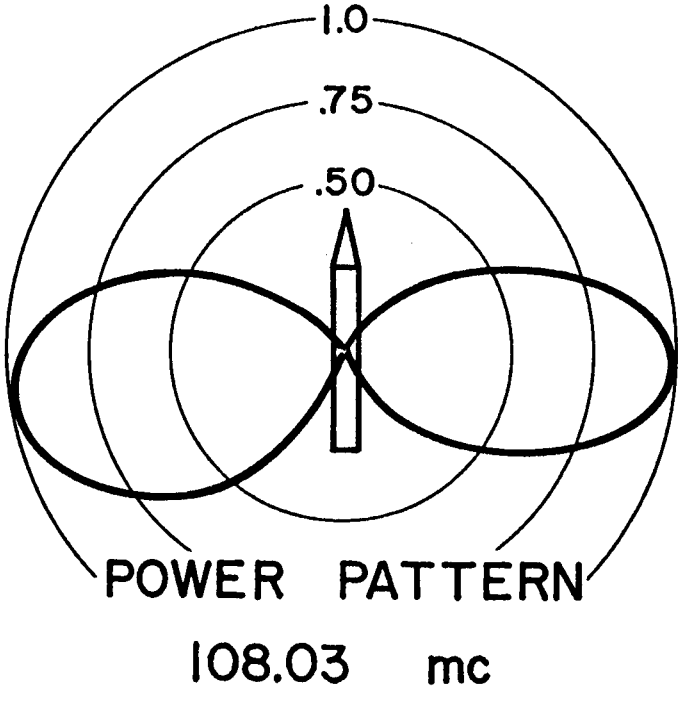

FIG. 4 Explorer IV antenna radiation patterns, which may be considered figures of revolution about the longitudinal axis.

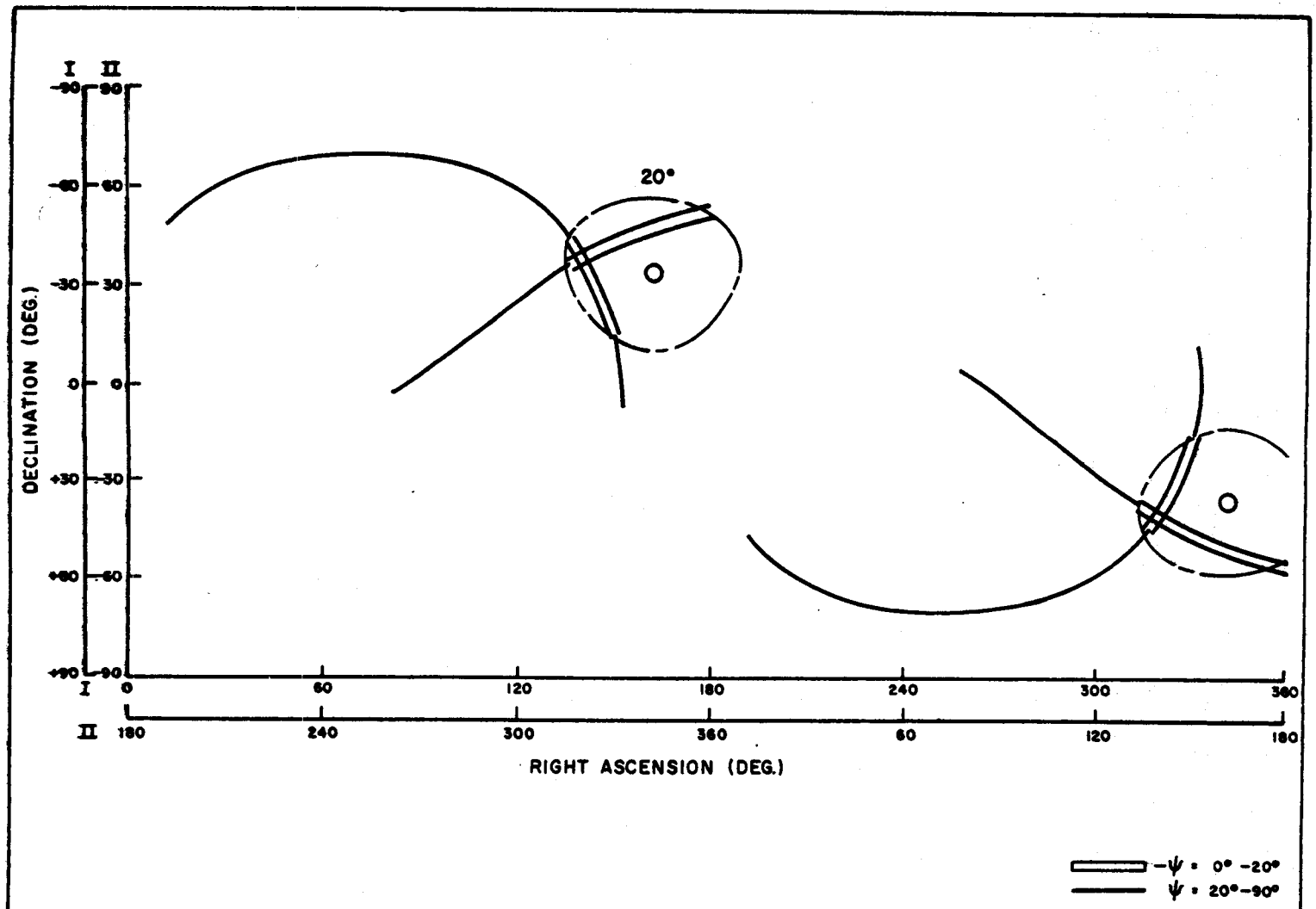

FIG. 5 Right ascension and declination of sight vector for passes during August 12, 1958.

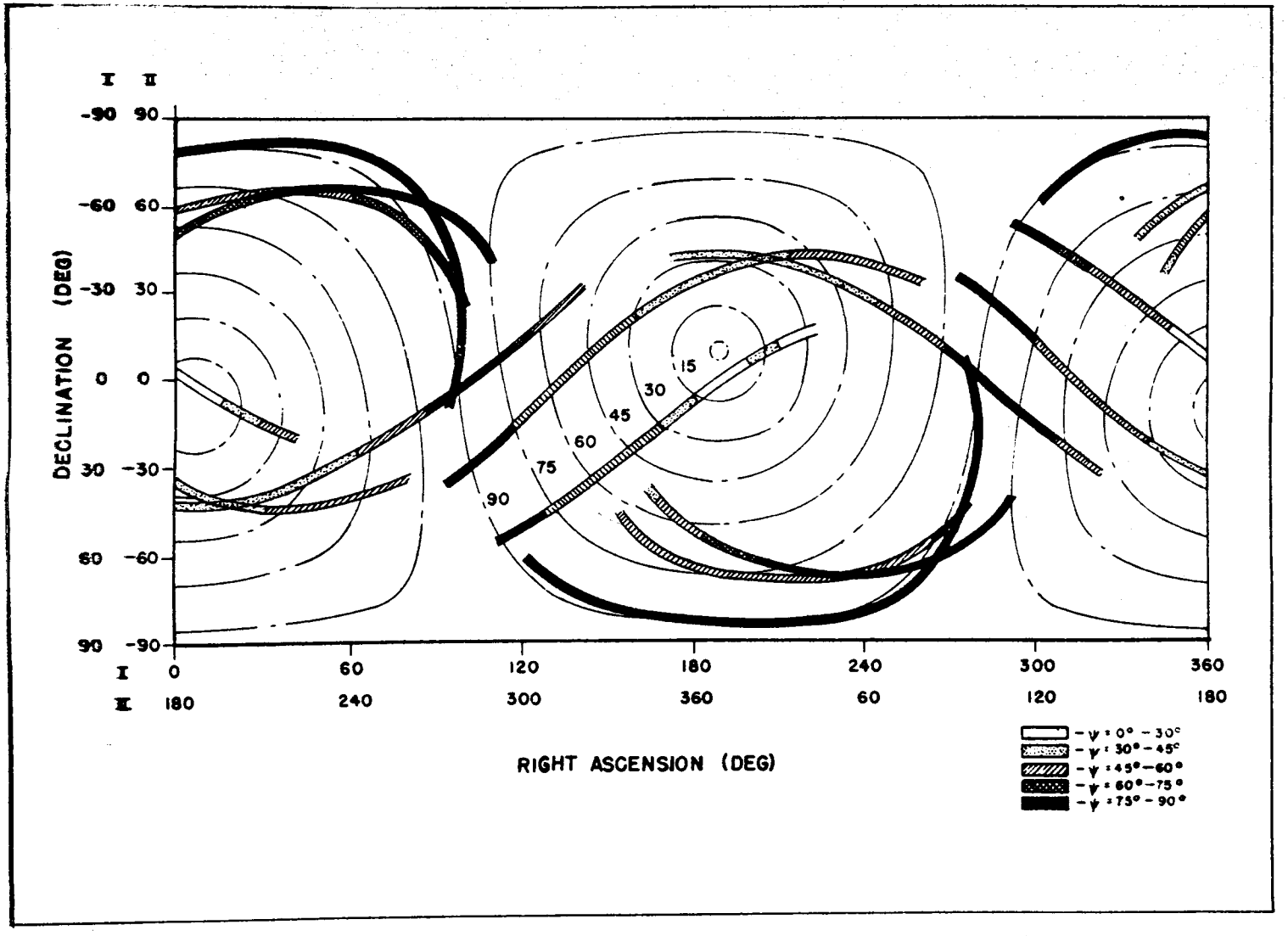

FIG. 6 Right ascension and declination of sight vector for passes during August 30, 1958. The types of signal strength patterns observed at various times are indicated by shading.

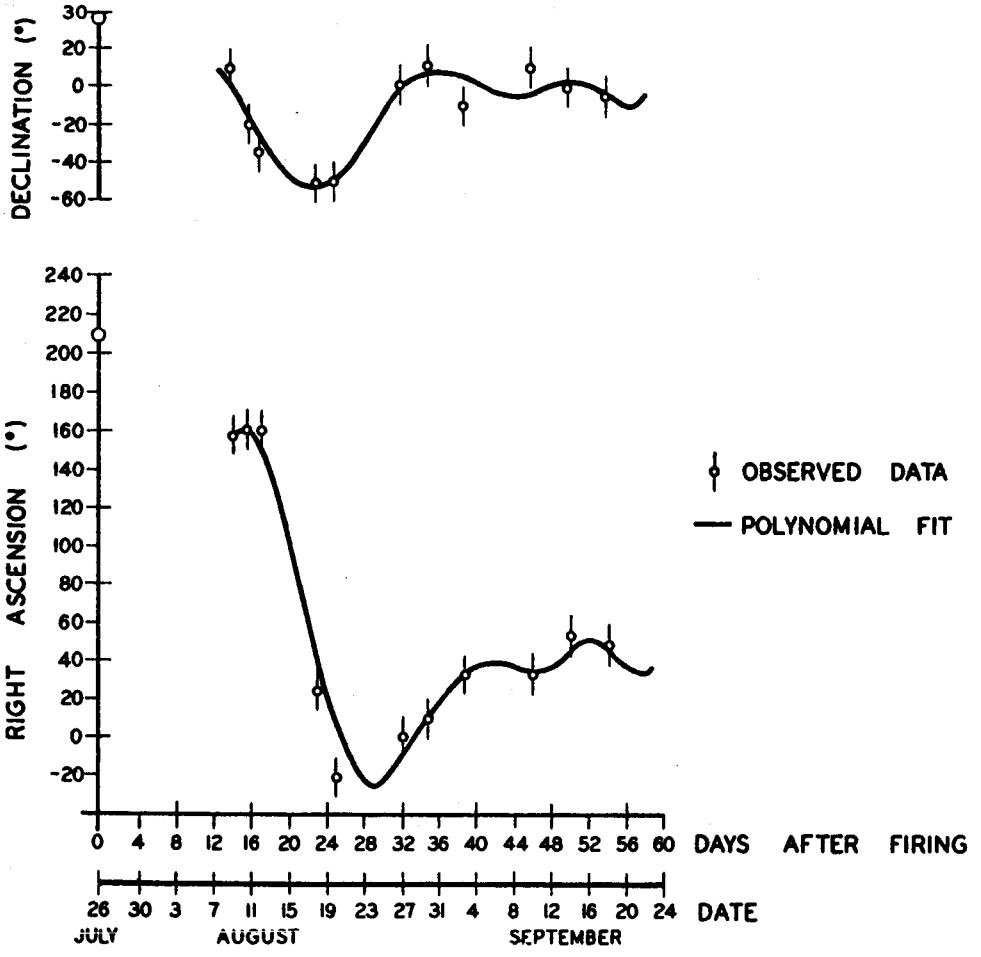

FIG. 7 Polynomial description of the right ascension and declination of the angular momentum vector.

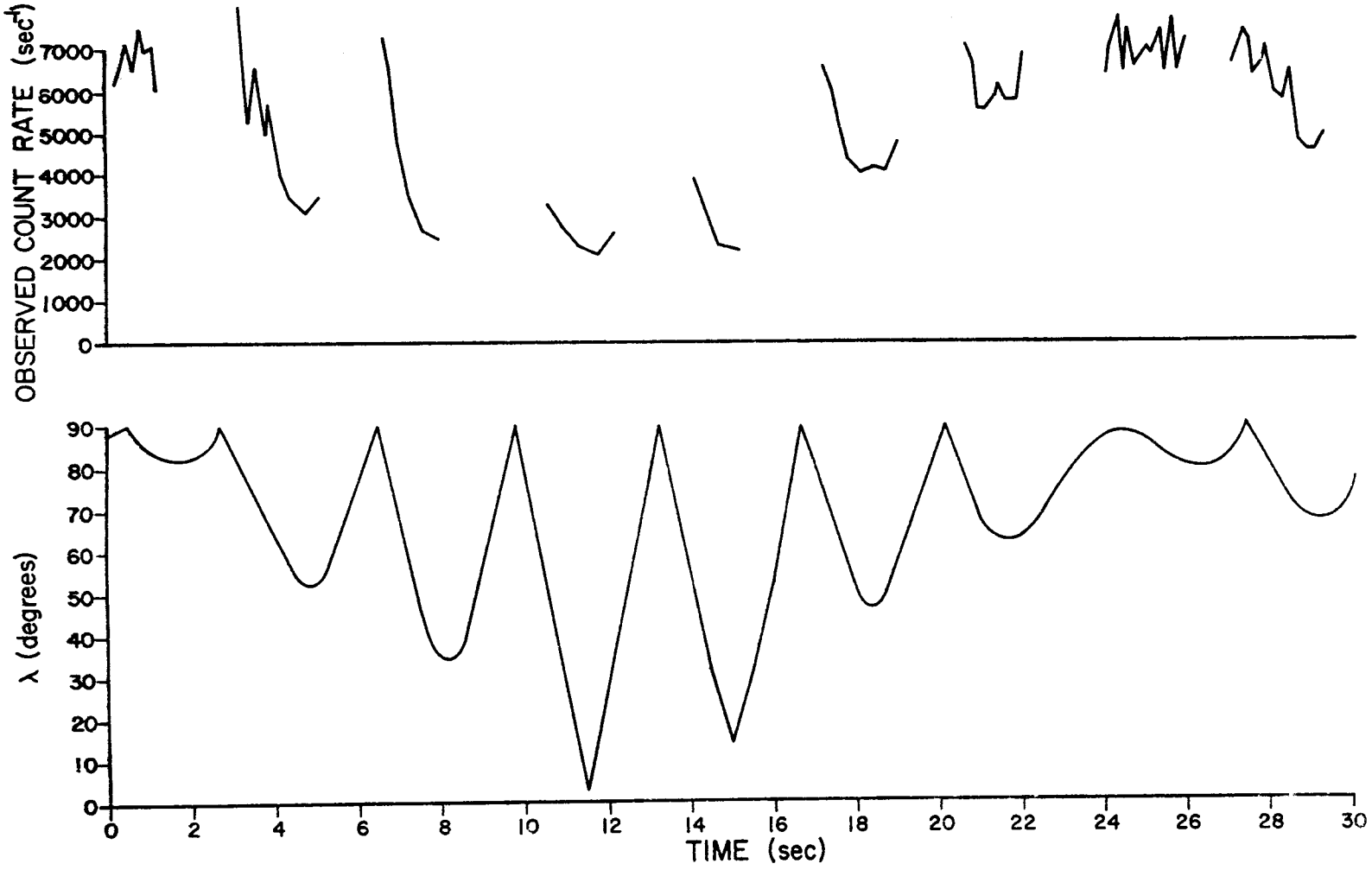

FIG. 8 Comparison of observed counting rates with the calculated λ during the interval 0500:00 to 0500:30 UT on August 30.

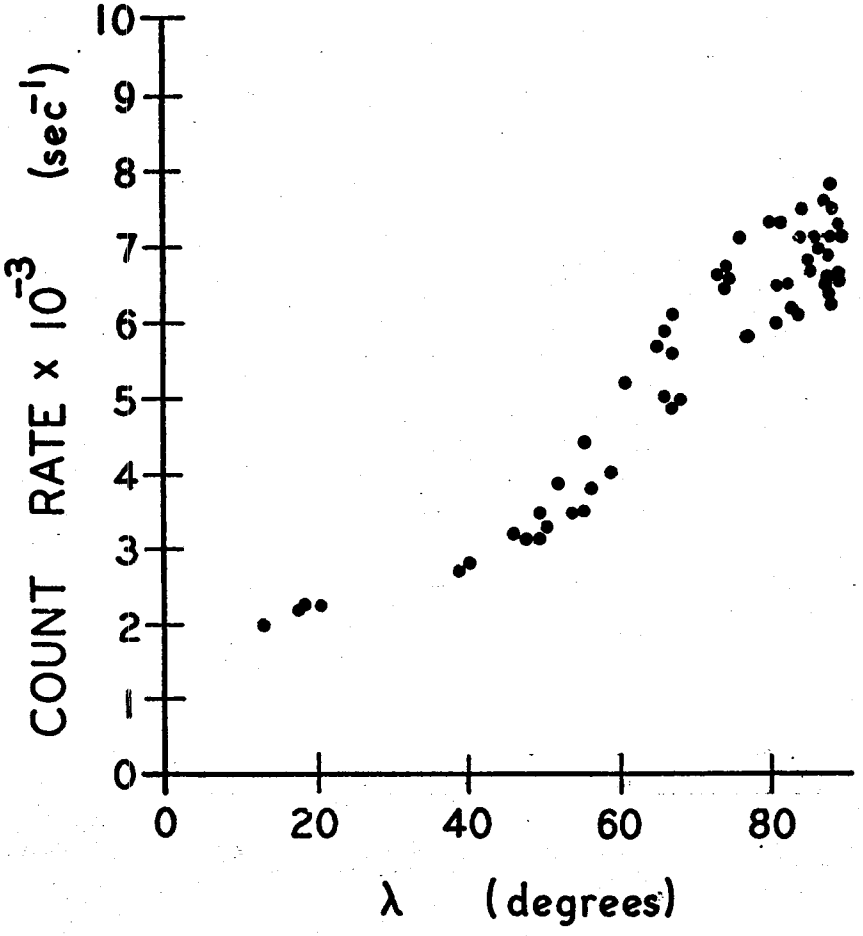

FIG. 9 Counting rate versus λ for 0500:00 to 0500:30 UT, August 30.

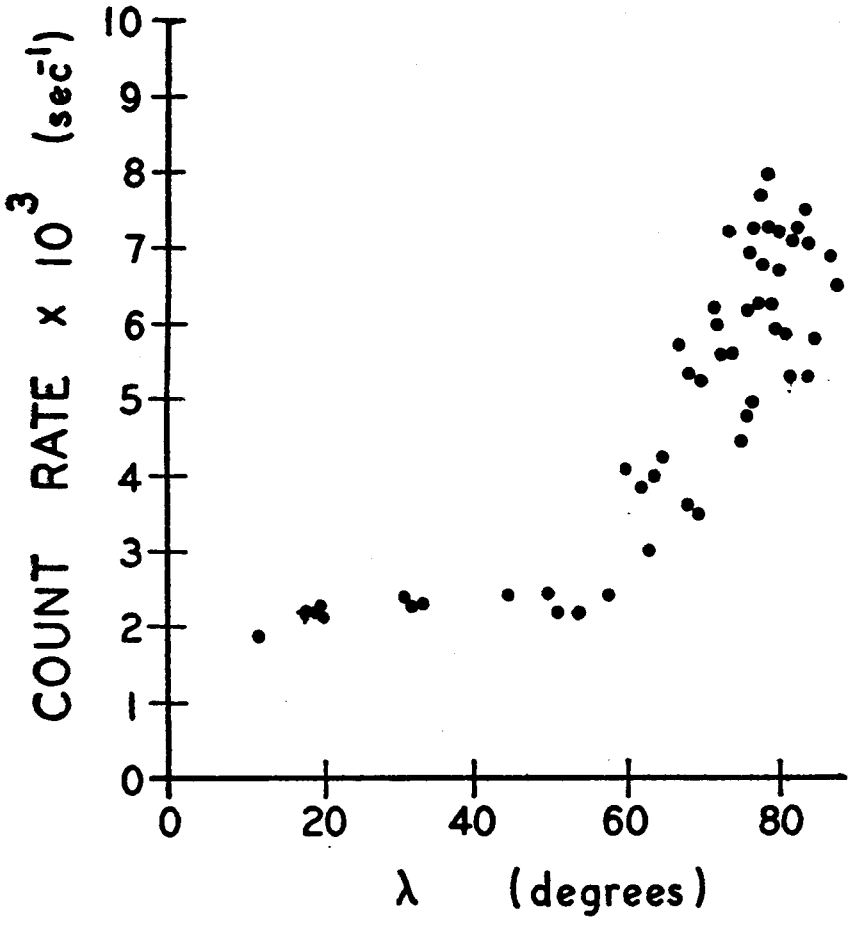

FIG. 10 Counting rate versus λ for 0500:30 to 0501:00 UT, August 30.

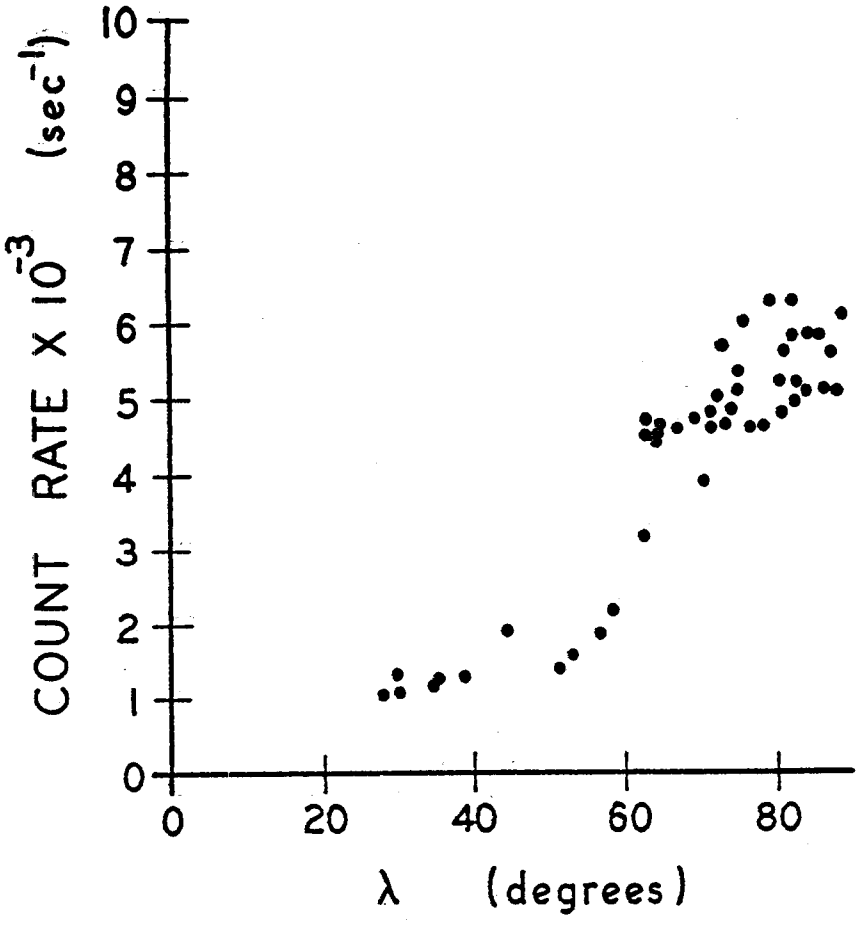

FIG. 11 Counting rate versus λ for 0502:30 to 0503:00, August 30.